Contrib. Astron. Obs. Skalnaté Pleso **56/1**, 69 – 74, (2026)
https://doi.org/10.31577/caosp.2026.56.1.69

Probing rotation in quasars using microlensing-induced line profile distortions

C. Fian

INAF – Osservatorio Astronomico di Trieste, via G.B. Tiepolo, 11, I-34143 Trieste, Italy, (E-mail: carina.fian@inaf.it)

Received: August 30, 2025; Accepted: November 19, 2025

Abstract. We present a novel method to derive rotation curves of the inner broad-line region (BLR) of lensed quasars with light-day spatial resolution. The approach exploits microlensing distortions of the broad emission lines (BELs), where the strength of the effect in the line wings traces the size of the emitting region at different velocities. We analyze the high-ionization lines Si IV and C IV in five gravitationally lensed quasars, measuring microlensing amplitudes across several velocity bins. Bayesian inference yields emission-region sizes, which we confront with a Keplerian disk model. We find a smooth, monotonic increase in microlensing with velocity, and the derived velocity–size relations are consistent with disk-like rotation. These results provide the first direct evidence for Keplerian motion in the innermost BLR of quasars.

Key words: Gravitational lensing: micro – quasars: emission lines

1. Introduction

Direct evidence on the kinematics of the broad emission line (BEL) regions in quasars is still limited. The observed line profiles cannot usually be linked unambiguously to specific motions, although a two-component model has often been invoked: line wings arising from the accretion disk and the line core from a more isotropic component (Fian et al., 2023). Separating these contributions, however, is challenging, and most studies rely on virial estimates that mainly probe the core of the lines (Kaspi et al., 2021). Several methods have been proposed to explore the inner broad-line region (BLR) kinematics, such as velocity-resolved reverberation mapping (De Rosa et al., 2018; Bentz et al., 2023) and spectro-astrometry with GRAVITY@VLTI (Gravity Collaboration et al., 2018). These techniques have revealed complex results and are usually limited to nearby active galactic nuclei with spatial resolutions of tens of light-days. Gravitational microlensing provides an alternative probe. It is sensitive to source size on light-day scales and can thus map the emission regions of quasars at cosmological distances. While previous microlensing studies have focused on entire emission lines, strong microlensing distortions in the wings of

some systems allow us to resolve the line profile into velocity bins. This enables the construction of experimental kinematic curves that relate velocity to emitting-region size. Here, we investigate the microlensing response in the high-ionization lines Si IV and C IV for five lensed quasars (SDSS J1001+5027, SDSS J1004+4112, HE 1104˘1805, SDSS J1206+4332, and SDSS J1339+1310). By comparing the observed microlensing signatures with predictions from a Keplerian disk model, we constrain the kinematics of the innermost BLR and test the hypothesis of disk-like rotation.

2. Data and observations

We compiled rest-frame ultraviolet spectra of gravitationally lensed quasars selected for clear microlensing signatures in the wings of the high-ionization lines Si IV λ1397 and/or C IV λ1549. Additional criteria required multi-epoch observations and sufficient signal-to-noise ratio in the relevant spectral range. The sample consists of one quadruply lensed quasar, SDSS J1004+4112 (z = 1.734), and four doubles: SDSS J1001+5027 (z = 1.838), HE 1104–1805 (z = 2.319), SDSS J1206+4332 (z = 1.789), and SDSS J1339+1310 (z = 2.243). The fully reduced spectra, collected from the literature, span multiple epochs over several years: six epochs for SDSS J1001+5027 (2003–2016), 21 epochs for SDSS J1004+4112 (2003–2018), seven epochs for HE 1104˘1805 (1993–2016), two epochs for SDSS J1206+4332 (2004, 2016), and eight epochs for SDSS J1339+1310 (2007–2017). For SDSS J1004+4112, only images A and B were used, since the long delays of images C and D ($\sim$ 2 and $\sim$ 4.5 years; Muñoz et al. 2022) might mix intrinsic variability with microlensing.

3. Methodology

For each quasar image, we first subtracted the local continuum by fitting a straight line to adjacent regions free of emission features. The line cores, expected to be largely unaffected by microlensing (Fian et al., 2018), were used as a reference: we normalized the cores of images A and B to remove macro-magnification and extinction effects (Guerras et al., 2013). Average normalized profiles were then constructed, and splines were fitted to the wings most susceptible to microlensing. Microlensing signatures were detected as follows: in SDSS J1001+5027, a modest enhancement of image B in the red C IV wing (blue wing excluded due to absorption); in SDSS J1004+4112, strong distortions with a magnified blue wing and demagnified red wing in image A (Hutsemékers et al., 2023; Fian et al., 2024b); in SDSS J1206+4332 and SDSS J1339+1310, strong magnification of image B in the red wings of both lines (Goicoechea & Shalyapin, 2016; Fian et al., 2021, 2024c), plus additional blue-wing magnification in SDSS J1206+4332; and in HE 1104–1805, modest magnification of the red wings in image A (Fian et al., 2021). To quantify differential microlensing

across velocities, we computed flux ratios between spline fits of the image pairs in 500 km s^{-1} bins, converted them into magnitudes, and sampled velocities between 3000–8000 km s^{-1}, yielding 11 independent measurements per line.

4. Microlensing simulations

To model microlensing of spatially extended sources, we employed the Fast Multipole Method–Inverse Polygon Mapping algorithm (FMM–IPM; Jiménez-Vicente & Mediavilla 2022), which combines the FMM approach for ray deflections with the IPM method for map generation. For each quasar image, we produced 3000×3000 pixel^2 magnification maps covering 100×100 Einstein radii^2, with a resolution of 0.30–0.40 light-days per pixel depending on the Einstein radius R_E. Stars of mass $0.3\,M_\odot$ were randomly distributed across the lens plane. The quasar emission regions were modeled with circular Gaussian profiles, $I(R) \propto \exp(-R^2/2r_s^2)$, convolved with the magnification maps. The relevant parameter is the half-light radius ($R_{1/2} = 1.18, r_s$), which largely determines microlensing results irrespective of the detailed brightness profile (Mortonson et al., 2005). Differential microlensing in the line wings between lensed images was used to infer emission-region sizes and thus probe BLR kinematics. Probabilities were computed by randomly placing the Gaussian sources on the maps and comparing the simulated and observed microlensing signals, following Guerras et al. (2013) and Fian et al. (2018, 2021).

5. Results and discussion

We examined microlensing magnification across velocity bins in the wings of Si IV and C IV, where contamination from other lines is minimal. This approach allows us to probe emission regions from several tens of light-days down to sub-light-day scales. A clear monotonic increase in microlensing with velocity is observed, consistent with high-velocity gas originating from more compact regions. A second key result is the agreement between velocity curves obtained from different wings or different lines in the same object, confirming the robustness of the method. We also find systematic asymmetries between red and blue wings: one wing may be magnified while the other is de-magnified, indicating that although both originate from similar-sized regions, they are not co-spatial. Finally, in several quasars (e.g., SDSS J1001+5027 and HE 1104˘1805) the velocity–size curves closely follow the expected Keplerian trend. In other systems, the curves flatten at high velocities, where size estimates are less reliable due to broad probability distributions. These deviations are within uncertainties and do not contradict the Keplerian hypothesis. Figure 1 illustrates the velocity-resolved microlensing signatures for one representative system in our sample. To improve statistical significance, we combined the velocity curves of all systems, scaling to a mean mass of $M_{\rm BH} \sin^2 i = 2.9 \times 10^7 M_\odot$. The stacked curve follows

near-Keplerian motion over 3000–5500 km s^{-1}, with mild flattening at higher velocities, where uncertainties increase. Overall, the results provide strong evidence for Keplerian rotation in the innermost BLR, directly linking this region to the accretion disk structure. A detailed discussion of these results is presented in Fian et al. (2024a).

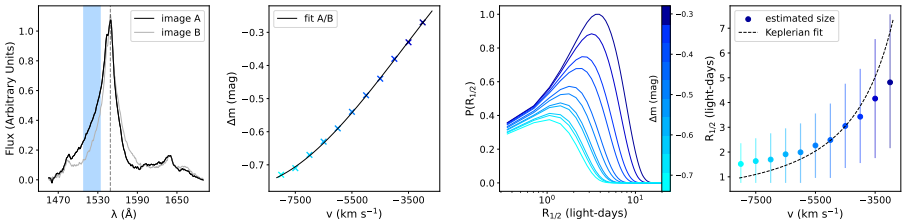

Figure 1. Kinematic responses to microlensing for SDSS J1004+4112. The left panel shows the average C IV line profiles for images A (black) and B (gray). The middle panels illustrate the magnitude differences between the images in the line wing and the probability density functions of the emitting region size. The rightmost panel displays the estimated sizes of different kinematic regions as a function of velocity, along with a Keplerian fit (dashed black line).

6. Conclusions

We obtained velocity-resolved microlensing magnification curves for the wings of the C IV and Si IV BELs in five lensed quasars. By linking microlensing strength to emitting-region size in each velocity bin, we derived velocity–size relations that reveal a smooth increase in magnification with velocity, consistent with high-velocity gas arising from more compact regions. We find strong consistency between curves obtained from red and blue wings of the same line, as well as from different lines in the same object, supporting the robustness of the method. Both individual systems and the composite curve align well with the predictions of a Keplerian disk, directly connecting the innermost BLR with the accretion disk structure. This represents the first direct evidence that the BLR follows Keplerian rotation over radii of $\sim 5\breve{}20$ light-days. Most notably, gravitational microlensing achieves an unprecedented spatial resolution - in some cases below one light-day - making it a uniquely powerful probe of quasar inner kinematics.

References

Bentz, M. C., Markham, M., Rosborough, S., et al., Velocity-resolved Reverberation Mapping of NGC 3227. 2023, *Astrophysical Journal*, **959**, 25, DOI:10.3847/1538-4357/ad08b8

De Rosa, G., Fausnaugh, M. M., Grier, C. J., et al., Velocity-resolved Reverberation Mapping of Five Bright Seyfert 1 Galaxies. 2018, *Astrophysical Journal*, **866**, 133, DOI:10.3847/1538-4357/aadd11

Fian, C., Guerras, E., Mediavilla, E., et al., Microlensing and Intrinsic Variability of the Broad Emission Lines of Lensed Quasars. 2018, *Astrophysical Journal*, **859**, 50, DOI:10.3847/1538-4357/aabc0d

Fian, C., Jiménez-Vicente, J., Mediavilla, E., et al., First Direct Evidence for Keplerian Rotation in Quasar Inner Broad-line Regions. 2024a, *Astrophysical Journal, Letters*, **972**, L7, DOI:10.3847/2041-8213/ad654d

Fian, C., Mediavilla, E., Motta, V., et al., Microlensing of the broad emission lines in 27 gravitationally lensed quasars. Broad line region structure and kinematics. 2021, *Astronomy and Astrophysics*, **653**, A109, DOI:10.1051/0004-6361/202039829

Fian, C., Muñoz, J. A., Forés-Toribio, R., et al., Probing the structure of the lensed quasar SDSS J1004+4112 through microlensing analysis of spectroscopic data. 2024b, *Astronomy and Astrophysics*, **682**, A57, DOI:10.1051/0004-6361/202347382

Fian, C., Muñoz, J. A., Jiménez-Vicente, J., et al., Revealing the inner workings of the lensed quasar SDSS J1339+1310: Insights from microlensing analysis. 2024c, *Astronomy and Astrophysics*, **689**, A129, DOI:10.1051/0004-6361/202450151

Fian, C., Muñoz, J. A., Mediavilla, E., et al., Revealing the structure of the lensed quasar Q 0957+561. III. Constraints on the size of the broad-line region. 2023, *Astronomy and Astrophysics*, **678**, A108, DOI:10.1051/0004-6361/202140975

Goicoechea, L. J. & Shalyapin, V. N., Gravitational lens system SDSS J1339+1310: microlensing factory and time delay. 2016, *Astronomy and Astrophysics*, **596**, A77, DOI:10.1051/0004-6361/201628790

Gravity Collaboration, Sturm, E., Dexter, J., et al., Spatially resolved rotation of the broad-line region of a quasar at sub-parsec scale. 2018, *Nature*, **563**, 657, DOI:10.1038/s41586-018-0731-9

Guerras, E., Mediavilla, E., Jimenez-Vicente, J., et al., Microlensing of Quasar Broad Emission Lines: Constraints on Broad Line Region Size. 2013, *Astrophysical Journal*, **764**, 160, DOI:10.1088/0004-637X/764/2/160

Hutsemékers, D., Sluse, D., Savić, Đ., & Richards, G. T., Microlensing of the broad emission line region in the lensed quasar J1004+4112. 2023, *Astronomy and Astrophysics*, **672**, A45, DOI:10.1051/0004-6361/202245490

Jiménez-Vicente, J. & Mediavilla, E., Fast Multipole Method for Gravitational Lensing: Application to High-magnification Quasar Microlensing. 2022, *Astrophysical Journal*, **941**, 80, DOI:10.3847/1538-4357/ac9e59

Kaspi, S., Brandt, W. N., Maoz, D., et al., Taking a Long Look: A Two-decade Reverberation Mapping Study of High-luminosity Quasars. 2021, *Astrophysical Journal*, **915**, 129, DOI:10.3847/1538-4357/ac00aa

Mortonson, M. J., Schechter, P. L., & Wambsganss, J., Size Is Everything: Universal Features of Quasar Microlensing with Extended Sources. 2005, *Astrophysical Journal*, **628**, 594, DOI:10.1086/431195

Muñoz, J. A., Kochanek, C. S., Fohlmeister, J., et al., The Longest Delay: A 14.5 yr Campaign to Determine the Third Time Delay in the Lensing Cluster SDSS J1004+4112. 2022, *Astrophysical Journal*, **937**, 34, DOI:10.3847/1538-4357/ac8877